Constitutive model for unsaturated fine-grained soils incorporating small strain stiffness

K. S. Wong & D. Mašín
Faculty of Science
Charles University in Prague, Czech Republic

ABSTRACT: In the paper, we present newly developed hydro-mechanical hypoplastic model for partially saturated soils incorporating small strain stiffness. The model is based on the existing hypoplastic model incorporating very small strain stiffness anisotropy. The model is combined with the hysteretic void ratio dependent water retention model and also with the approach enabling predictions of the very small strain stiffness and stiffness degradation curves. It is demonstrated by simulation of experimental data on completely decomposed tuff from Hong-Kong that the model predicts properly the very small strain stiffness dependency on mean effective stress, void ratio and degree of saturation. Central to correct predictions of suction history dependent stiffness degradation curves is consideration of the dependency of the elastic range size on suction.

1 INTRODUCTION

Soil stiffness at small strains (0.001% to 1%) is a key parameter for predicting ground deformations and dynamic responses of many earth structures such as retaining walls, foundations and tunnels. Moreover, correct consideration of stiffness development is crucial for capturing cyclic loading phenomena, induced for example by enviromental effects during wetting and drying cycles. Over the decades, many constitutive models have been developed and validated for modelling small strain stiffness in saturated soils. However, less research has been devoted to modelling shear stiffness at small strain in unsaturated soils and the overall non-linear stress-strain response from the very small strain stiffness up to the failure. In this paper, we present a new coupled hydro-mechanical hypoplastic model for partially saturated soils. The model inherits some features from the earlier hypoplastic models and, in addition, it incorporates small strain stiffness dependent on stress and suction history and hysteretic water retention curve.

2 MODEL FORMULATION

2.1 *Basic hydro-mechanical hypoplastic model*

Before incorporating the very small strain stiffness effects, we first needed to formulate the underlining hypoplastic model capable of predicting large strain behaviour and asymptotic states. The model is an evolution of the mechanical hypoplastic model for unsaturated soils by Mašín & Khalili (2008) and water retention model by Mašín (2010). These models were evaluated by D'Onza et al. (2011), demonstrating their good predictive capabilities. The models have been evolved in two ways. First, the new formulation is based on an explicit hypoplastic formulation by Mašín (2012), leading to more freedom in further model enhancements (such as the incorporation of stiffness anisotropy, see Mašín & Rott 2013). Second, a hysteretic water retention model schematised in Fig. 1 has been adopted.

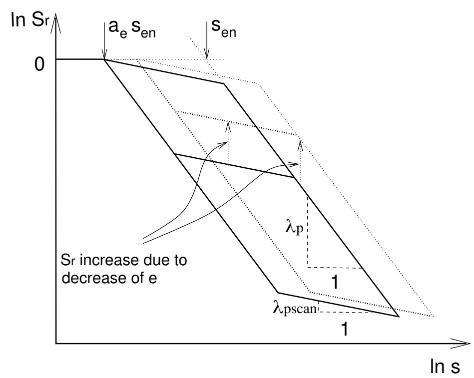

Figure 1: Hysteretic water retention curve adopted in the proposed model.

In the model formulation, parameter a_e defines the ratio of air expulsion and air entry values of suction (see Fig. 1). The water retention curve formulation is based on a new state variable denoted as a_{scan}, which is defined as

$$a_{scan} = \frac{s - s_W}{s_D - s_W} \tag{1}$$

In Eq. (1), s_D is suction at the main drying curve and s_W at the main wetting curve corresponding to the current degree of saturation S_r. It follows from (1) and a_e definition that s_D may be expressed as

$$s_D = \frac{s_{en}}{s_e} s \tag{2}$$

with

$$s_e = s_{en} \left(a_e + a_{scan} - a_e a_{scan} \right) \tag{3}$$

The hysteretic model can then be defined using the rate equation for a_{scan}, such that for $s > a_e s_{en}$

$$\dot{a}_{scan} = \frac{1 - r_\lambda}{s_D (1 - a_e)} \dot{s} \tag{4}$$

where the ratio r_λ is defined as

$$r_\lambda = \begin{cases} 1 & \text{for} \quad s = s_D \quad \text{and} \quad \dot{s} > 0 \\ 1 & \text{for} \quad s = a_e s_D \quad \text{and} \quad \dot{s} < 0 \\ \frac{\lambda_{pscan}}{\lambda_p} & \text{otherwise} \end{cases} \tag{5}$$

The meaning of variables λ_p and λ_{pscan} is clear from Fig. 1. If $s \leq a_e s_{en}$, then $a_{scan} = 0$. Note that $\partial a_{scan} / \partial e = 0$ is assumed. Thus, the position along scanning curve does not influence the dependency of S_r on void ratio calculated using the model from Mašín (2010). Finite expression for S_r of the hysteretic model then reads simply:

$$S_r = \begin{cases} 1 & \text{for} \quad s \leq a_e s_{en} \\ \left(\frac{s_e}{s} \right)^{\lambda_p} & \text{for} \quad s > a_e s_{en} \end{cases} \tag{6}$$

Further modifications of the basic hypoplastic model by Mašín & Khalili (2008) are needed to incorporate hysteretic void-ratio dependent water retention curve. First of all, we need to consider the dependency of the effective stress on void ratio. In the new model, Bishop effective stress equation is considered, with the χ formulation following the work by Khalili & Khabbaz (1998). Thus, for $S_r < 1$,

$$\chi = \left(\frac{s_e}{s} \right)^{\gamma} \tag{7}$$

and $\chi = 1$ otherwise. Note that some authors advocate different modelling approach (Sheng et al. 2008). Unlike in the original model, in which s_e is considered to be material constant independent of e, the effective stress rate equation of the new model reads

$$\mathring{\boldsymbol{\sigma}} = \mathring{\boldsymbol{\sigma}}^{net} - \mathbf{1} \frac{\partial (\chi s)}{\partial t} = \mathring{\boldsymbol{\sigma}}^{net} - \mathbf{1} \left[\frac{\partial (\chi s)}{\partial s} \dot{s} + \frac{\partial (\chi s)}{\partial e} \dot{e} \right] \tag{8}$$

where $\boldsymbol{\sigma}$ is the effective stress, $\boldsymbol{\sigma}^{net}$ is net stress and the circle symbol ($\mathring{\boldsymbol{\sigma}}$) denotes objective rate. The derivative $\partial \chi s / \partial s$ in the hysteretic water retention curve formulation can be expressed using the variable r_λ as

$$\frac{\partial (\chi s)}{\partial s} = (1 - \gamma r_\lambda) \, \chi \tag{9}$$

The derivative $\partial \chi s / \partial e$ then follows from the Mašín (2010) model.

The second required modification which must be considered in the model is based on the fact that also variables controlling position $N(s)$ and slope $\lambda^*(s)$ of water retention curve are void ratio dependent, as both are expressed in terms of s_e:

$$N(s) = N + n_s \left\langle \ln \left(\frac{s}{s_e} \right) \right\rangle \tag{10}$$

$$\lambda^*(s) = \lambda^* + l_s \left\langle \ln \left(\frac{s}{s_e} \right) \right\rangle \tag{11}$$

The effective slope of normal compression line λ^*_{act}, entering the hypoplastic formulation, thus differs from $\lambda^*(s)$. The value of λ^*_{act} can be expressed explicitly by considering the $\partial s_e / \partial e$ expression of the Mašín (2010) model.

For space reasons, all equations of the coupled hypoplastic model cannot be included in this paper, the readers are referred to the journal publication by Wong & Mašín (2013).

2.2 *Formulation for the very small strain shear modulus*

Incorporation of small strain stiffness and its evolution into a constitutive model requires three main components: a model for large strain response, reference value of the very small strain stiffness and a model describing the stiffness degradation at small strains. The first component has been discussed in Sec. 2.1 and the last one will be described in Sec. 2.3. In this section, we describe the adopted formulation for the very small strain shear modulus G_0. The formulation has been developed by Wong et al. (2014) and it reads:

$$G_0 = p_r A_g \left(\frac{p}{p_r} \right)^{n_g} e^{(-m_g)} S_r^{(-k_g/\lambda_p)} \tag{12}$$

$$G_0 = p_r A_g \left(\frac{p}{p_r} \right)^{n_g} e^{(-m_g)} \left(\frac{s}{s_e} \right)^{k_g} \tag{13}$$

where p is mean effective stress calculated using χ factor of Eq. (7), which can also be expressed for the adopted water retention model as

$$\chi = S_r^{(\gamma/\lambda_p)} \tag{14}$$

(see D'Onza et al. 2011). In Eq. (12), p_r is a reference pressure of 1 kPa. A_g, n_g, m_g and k_g are model parameters controlling G_0 magnitude and its dependency on mean effective stress, void ratio and degree of saturation.

In developing Eq. (12), we considered the G_0 formulation of the cemented clays by Trhlíková et al. (2012). They found that G_0 does not depend on mean effective stress and soil relative density only, but also on the level of inter-particle cementation. Similarly, in the proposed G_0 formulation for partially saturated soils, G_0 depends on the mean effective stress, void ratio (which is an approximate measure of the number inter-particle contacts), and degree of saturation S_r. As suggested by Gallipoli et al. (2003), it is the number of water menisci, rather than the actual value of matric suction, which is controlling the water menisci bonding effect in partially saturated soils. The number of water menisci per unit volume of solid fraction is measured by degree of saturation, a function of which forms the last term in our G_0 formulation.

The Equation (12) predicts both the effects on G_0 of mechanical hysteresis (thanks to the void ratio term) and of hydraulic hysteresis (thanks to the S_r term combined with the hysteretic water retention curve formulation). Example evaluation of the model will be shown in Sec. 3, more details can be found in Wong et al. (2014).

2.3 *Hypoplastic model incorporating small strain stiffness*

Small strain stiffness effects have been incorporated into the hypoplastic models for saturated soils by means of the intergranular strain concept proposed by Niemunis & Herle (1997). In this paper, we describe a modification of this concept to predict small strain stiffness of partially saturated soils. The modification has been proposed by Wong & Mašín (2013).

The general rate equation of hypoplastic model reads (Mašín & Khalili 2008):

$$\overset{\circ}{\boldsymbol{\sigma}} = f_s \left(\boldsymbol{\mathcal{L}} : \dot{\boldsymbol{\epsilon}} + f_d \mathbf{N} \|\dot{\boldsymbol{\epsilon}}\| \right) + f_u \mathbf{H} \tag{15}$$

where $\boldsymbol{\mathcal{L}}$ and $\mathbf{N}$ are fourth- and second-order constitutive tensors respectively, $\dot{\boldsymbol{\epsilon}}$ is the Euler stretching tensor, $\|\dot{\boldsymbol{\epsilon}}\|$ is the Euclidian norm of $\dot{\boldsymbol{\epsilon}}$ and $\mathbf{H}$ is the second-order tensor enabling to predict wetting-induced collapse. f_s, f_d and f_u are three scalar factors controlling the effects of effective stress and overconsolidation ratio on model response.

The general rate equation of the small strain stiffness model reads

$$\overset{\circ}{\boldsymbol{\sigma}} = \boldsymbol{\mathcal{M}} : \dot{\boldsymbol{\epsilon}} + f_u \mathbf{H} \tag{16}$$

In the very small strain range,

$$\boldsymbol{\mathcal{M}} = m_R f_s \boldsymbol{\mathcal{L}} \tag{17}$$

where m_R is a variable controlling very small strain stiffnes magnitude. It is calculated to ensure the very small strain shear modulus is expressed using Eq. (12).

In the small strain range, $\boldsymbol{\mathcal{M}}$ is found by an interpolation between the limitting cases of (15) and (17). The interpolation is taken over from Niemunis & Herle (1997), see also Mašín (2005).

The size of the elastic range is in the original intergranular strain model defined by the parameter R. Evaluation of the model using experimental data on small strain stiffness of partially saturated soils revealed that the size of the elastic range depends on the current value of the ratio s/s_e (that is, it depends on current degree of saturation). We can again recall similarity with the behaviour of cemented soils. As observed, among others, by Sharma & Fahey (2004), the amount of cementing agent increases the size of the elastic range. In the small strain stiffness hypoplastic model, the size of the elastic range, denoted as $R(s)$, is calculated as

$$R(s) = R + r_m \ln \frac{s}{s_e} = R - \frac{r_m}{\lambda_p} \ln S_r \tag{18}$$

where r_m is a model parameter controlling the dependency of $R(s)$ on the ratio s/s_e (and thus on S_r).

In the new formulation, $R(s)$ depends on both suction and void ratio. Time derivative of (18) yields

$$\dot{R}(s) = r_m \left(r_\lambda \frac{\dot{s}}{s} + \frac{\gamma}{e \lambda_{psu}} \dot{e} \right) \tag{19}$$

where λ_{psu} is a variable specified in the Mašín (2010) model. To consider the fact that suction and void ratio influence the size of the elastic range, rate formulation of the intergranular strain is adjusted such that for $\hat{\boldsymbol{\delta}} : \mathbf{D} > 0$, $s > s_e$ and $\dot{R}(s) < 0$

$$\overset{\circ}{\boldsymbol{\delta}} = \left(\boldsymbol{\mathcal{I}} - \hat{\boldsymbol{\delta}} \otimes \hat{\boldsymbol{\delta}} \rho^{\beta_r} \right) : \mathbf{D} + \boldsymbol{\delta} \frac{\dot{R}(s)}{R(s)} \tag{20}$$

For other cases, the original formulation remains unchanged. In Eq. (20), $\boldsymbol{\delta}$ is the intergranular strain. For definition of the other variables appearing in Eq. (20), the readers are referred to Niemunis & Herle (1997).

3 EVALUATION OF THE MODEL

In this section, the proposed constitutive model is evaluated using experimental data on completely decomposed tuff (CDT) from Hong-Kong. The material tested was a CDT extracted from a deep excavation site at Fanling, Hong Kong (Ng & Yung 2008). The material would be described as clayey silt (ML) according to the Unified Soil Classification System. The material was yellowish-brown, slightly plastic, with a very small percentage of fine and coarse sand. The material used in the study has been recompacted by static compaction at initial water content of about 16.3% and dry density of about 1760 kg/m^3. The average initial suction of the specimens after compaction was 95 kPa. For details on the tested soil, see Ng & Yung (2008).

3.1 *Evaluation of the very small strain shear modulus predictions*

Very small strain shear moduli measurements investigated using bender element tests have been reported by Ng & Yung (2008) and Ng et al. (2009). Different types of experiments have been performed and simulated:

1. Isotropic compression tests at constant matric suction. Four different experiments have been performed and simulated, at matric suctions of 0, 50, 100 and 200 kPa.

2. Drying-wetting tests at the isotropic stress state and constant net mean stress. Two tests with net mean stresses of 110 kPa and 300 kPa have been simulated.

Experimental measurements of G_0 during the constant suction isotropic compression tests are shown in Fig. 2. The parameters A_g, m_g, n_g and k_g have been calibrated by a trial and error procedure to fit the very small strain stiffness data at $s = 0$, 50 and 100 kPa. Simulations are shown in Fig. 3, revealing that both the dependency of G_0 on mean effective stress and suction has been predicted properly by the model. Model parameters are in Tab. 3.1.

Table 1: Parameters of the proposed model adopted in all simulations.

basic model	φ_c 38°	λ^* 0.053	κ^* 0.005	N 0.76	ν_{pp} 0.25	α_G 1
unsat. mechanical	n_s 0	l_s 0	m (n/a)			
WRC model	s_{e0} 67 kPa	e_0 0.568	λ_{p0} 0.6	a_e 0.5		
G_0 model	A_g 4220	n_g 0.55	m_g 0.9	k_g 0.2		
intergr. strain model	R 10^{-4}	β_r 2	χ 1	m_{rat} 1	r_m 8x10^{-5}	

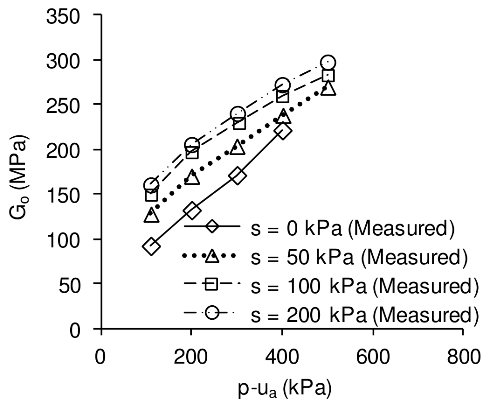

Figure 2: G_0 dependency on net mean stress during constant suction isotropic compression tests (data by Ng & Yung, 2008).

For model validation, drying-wetting tests at constant net stress have been simulated. Experimental measurements are shown in Fig. 4a. The water retention curve was significantly hysteretic (see Fig. 6 in Sec. 3.2). In our model, the hysteresis effects on

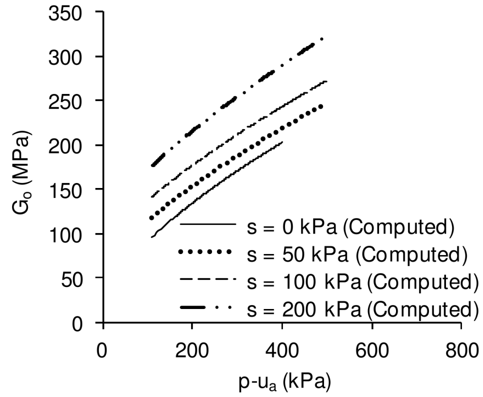

Figure 3: G_0 dependency on net mean stress during constant suction isotropic compression tests, model simulations.

G_0 are considered by allowing for the dependency of G_0 on void ratio, effective mean stress and degree of saturation (in combination with hysteretic mechanical and water retention models). G_0 dependency on suction predicted by the model during wetting-drying tests is shown in Fig. 4b. The model well represents the hysteretic response thanks to the hysteretic water retention curve (Fig. 1). Unlike the model, the experimental data reveal hysteresis in the suction range below 50 kPa. This is not predicted by the model, due to the inaccurate representation of the wetting branch of water retention curve in the low suction range (see Fig. 6).

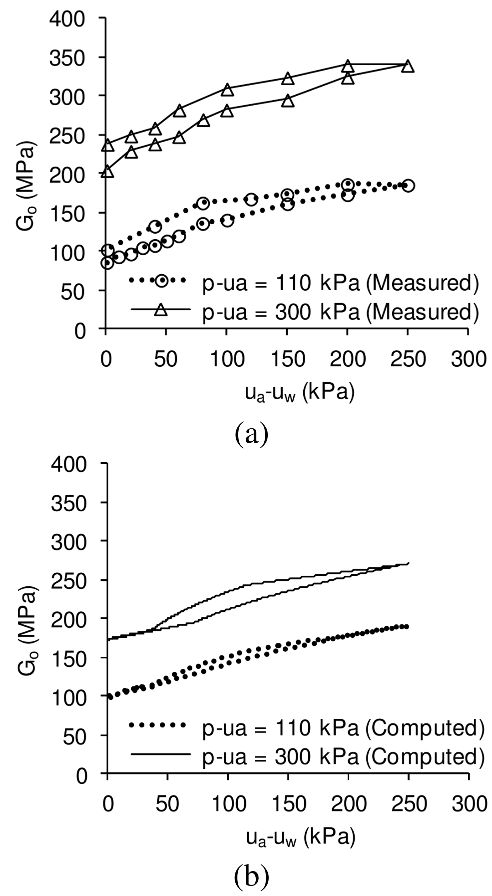

Figure 4: G_0 dependency on suction during constant net mean stress wetting-drying tests. (a) experimental data by Ng et al., (2009), (b) model simulations.

3.2 *Hypoplastic model incorporating small strain stiffness*

To evaluate the model predictions in the small strain range including the dependency of shear modulus degradation curve on stress and suction history, we adopted experimental data by Ng & Xu (2012) and Xu (2011). They used soil from the same locality as the soil adopted in G_0 measurements. Different samples were, however, used in the two investigations, which implied minor differences in soil properties caused by the soil natural variability.

The following experiments were adopted for the model evaluation:

1. The first set of experiments has been designed to investigate the effect of suction magnitude on small strain stiffness. The samples were loaded isotropicaly under constant suction from the as-compacted state of $s = 95$ kPa and $p^{net} = 0$ kPa until the net mean stress of 100 kPa. Subsequently, suction was increased to either 150 or 300 kPa or decreased to 1 kPa. Then, the samples were sheared under constant p^{net} conditions and stiffness degradation curve was recorded. The stress-suction paths are clear from Fig. 5. The three experiments described are represented by paths ABS_1C_1, ABS_2C_2 and ABS_3C_3.

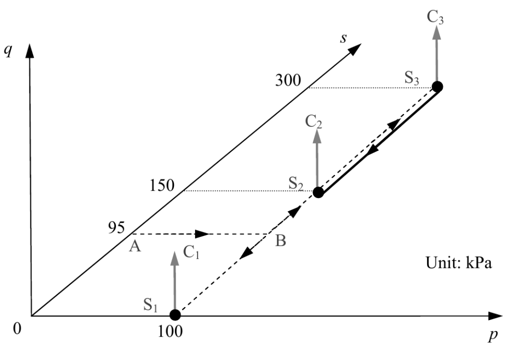

Figure 5: Stress-suction histories adopted in small strain stiffness tests (from Xu, 2011).

2. The second set of experiments has been designed to investigate the effect of suction history on small strain stiffness. The test ABS_2C_2 described previously has been supplemented by the test $ABS_2S_3S_2C_2$. The shear stage of the two tests has thus been performed at the same suction levels of $s = 150$ kPa. The immediate past suction history of one test was drying from 95 to 150 kPa, while the history of the other test was wetting from 300 kPa to 150 kPa.

To simulated the tests with the proposed model, all the model parameters had to be calibrated first. Detailed description of the calibration procedure is out of the length limits for the present paper; the parameters are summarised in Table 3.1. Central to the present developments is calibration of water retention curve. Model predictions are shown in Fig. 6. The model represents the basic features of hysteretic hydraulic behaviour, it is however clear that the bi-linear representation does not fit well the experimental data in the low suction range.

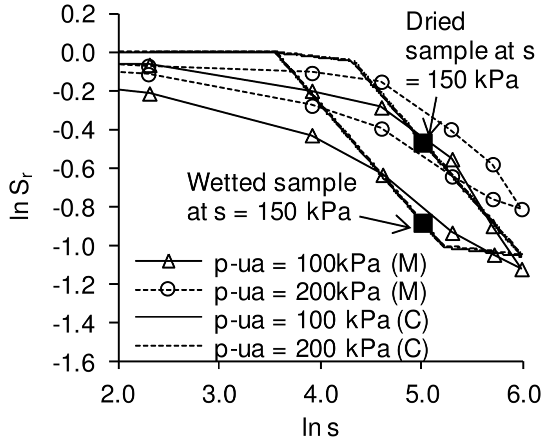

Figure 6: Hysteretic water retention curve. Experimental data by Ng and Xu (2012) and model predictions with indication of the initial states of the two s=150 kPa experiments.

Figure 7a shows predictions by the model for the first set of experiments adopting suction-independent size of the elastic range R (calibrated using the test at saturated conditions), that is adopting Eq. (18) with $r_m = 0$. Clearly, such a model underpredicts significantly stiffness in the unsaturated state. Predictions are significantly improved if the size of the elastic range is allowed to increase with decreasing degree of saturation (Fig. 7b).

Simulations of the second set of experiments are shown in Fig. 8. The model predicts properly the trend in the depndency of shear stiffness degradation on suction history. The reason for this model capability may be explained with the aid of Fig. 6. As soil state of one test is at the main drying branch of water retention curve, while state of the other test is at the main wetting branch, the two samples are characterised by different values of the ratio s/s_e (although suction is the same in both cases). As s/s_e enters the expression for the elastic range size $R(s)$ (Eq. (18)), the elastic range of the recently wetted samples is larger than the elastic range of the recently dried sample.

4 SUMMARY AND CONCLUSIONS

In the paper, we presented the coupled hydro-mechanical hypoplastic model for partially saturated soils incorporating small strain stiffness. Fundamental features of the model formulation were described, followed by evaluation of those features novel with respect to the existing models. In particular, we presented predictive capability of the very small strain stiffness model defined in terms of mean effective stress, void ratio and degree of saturation. Subsequently, the small strain stiffness degradation model was evaluated. It was shown that crucial for correct

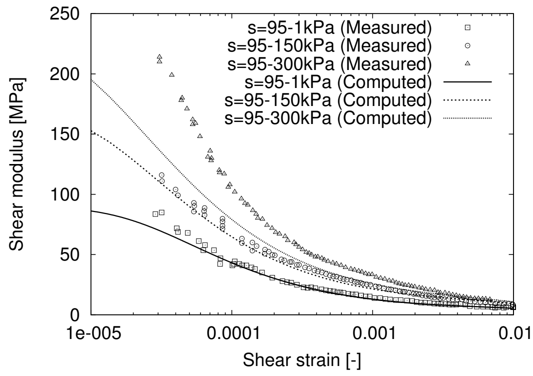

(a)

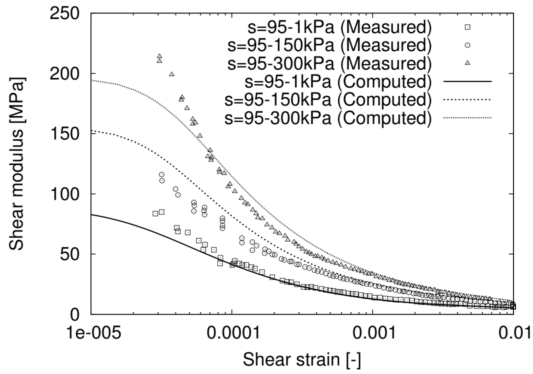

(b)

Figure 7: Stiffness degradation curves from the first set of experiments, experimental data by Ng and Xu (2012) compared with the model predictions. (a) model with constant $R(s)$, (b) model with $R(s)$ dependent on suction.

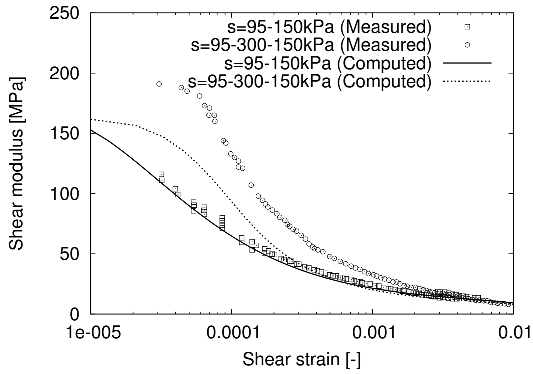

(a)

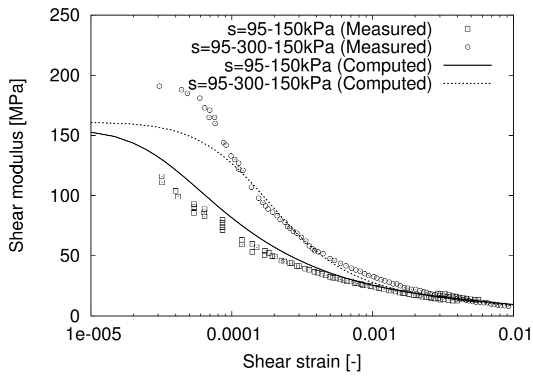

(b)

Figure 8: Stiffness degradation curves from the second set of experiments, experimental data by Ng and Xu (2012) compared with the model predictions. (a) model with constant $R(s)$, (b) model with $R(s)$ dependent on suction.

predictions was consideration of the dependency of the elastic range size on suction.

ACKNOWLEDGEMENT

The research has been funded by the grant No. 14-32105S of the Czech Science Foundation.

REFERENCES

D'Onza, F., D. Gallipoli, S. Wheeler, F. Casini, J. Vaunat, N. Khalili, L. Laloui, C. Mancuso, D. Mašín, M. Nuth, M. Pereira, & R. Vassallo (2011). Benchmark of constitutive models for unsaturated soils. *Géotechnique 61*(4), 283–302.

Gallipoli, D., A. Gens, R. Sharma, & J. Vaunat (2003). An elasto-plastic model for unsaturated soil incorporating the effects of suction and degree of saturation on mechanical behaviour. *Géotechnique 53*(1), 123–135.

Khalili, N. & M. H. Khabbaz (1998). A unique relationship for χ for the determination of the shear strength of unsaturated soils. *Géotechnique 48*(2), 1–7.

Mašín, D. (2005). A hypoplastic constitutive model for clays. *International Journal for Numerical and Analytical Methods in Geomechanics 29*(4), 311–336.

Mašín, D. (2010). Predicting the dependency of a degree of saturation on void ratio and suction using effective stress principle for unsaturated soils. *International Journal for Numerical and Analytical Methods in Geomechanics 34*, 73–90.

Mašín, D. (2012). Clay hypoplasticity with explicitly defined asymptotic states. *Acta Geotechnica 8*(5), 481–496.

Mašín, D. & N. Khalili (2008). A hypoplastic model for mechanical response of unsaturated soils. *International Journal for Numerical and Analytical Methods in Geomechanics 32*(15), 1903–1926.

Mašín, D. & J. Rott (2013). Small strain stiffness anisotropy of natural sedimentary clays: review and a model. *Acta Geotechnica, DOI:10.1007/s11440-013-0271-2*.

Ng, C. W. W. & J. Xu (2012). Effects of current suction ratio and recent suction history on small-strain behaviour of an unsaturated soil. *Canadian Geotechnical Journal 49*, 226–243.

Ng, C. W. W., J. Xu, & S. Y. Yung (2009). Effects of wetting-drying and stress ratio on anisotropic stiffness of an unsaturated soil at very small strains. *Canadian Geotechnical Journal 46*, 1062–1076.

Ng, C. W. W. & S. Y. Yung (2008). Determination of the anisotropic shear stiffness of an unsaturated decomposed soil. *Géotechnique 58*(1), 23–35.

Niemunis, A. & I. Herle (1997). Hypoplastic model for cohesionless soils with elastic strain range. *Mechanics of Cohesive-Frictional Materials 2*(4), 279–299.

Sharma, S. S. & M. Fahey (2004). Deformation characteristics of two cemented calcareous soils. *Canadian Geotechnical Journal 41*, 1139–1151.

Sheng, D., D. G. Fredlund, & A. Gens (2008). A new modelling approach for unsaturated soils using independent stress variables. *Canadian Geotechnical Journal 45*, 511–534.

Trhlíková, J., D. Mašín, & J. Boháč (2012). Modelling of the small strain behaviour of cemented soils. *Géotechnique 62*(10), 943–947.

Wong, K. S. & D. Mašín (2013). Coupled hydro-mechanical hypoplastic model for partially saturated soils incorporating small strain stiffness. *(in preparation)*.

Wong, K. S., D. Mašín, & C. W. W. Ng. (2014). Modelling of shear stiffness of unsaturated fine grained soils at very small strains. *Computers and Geotechnics 56*, 28–39.

Xu, J. (2011). *Experimental study of effects of suction history and wetting-drying on small strain stiffness of an unsaturated soil*. Ph. D. thesis, The Hong Kong University of Science and Technology.